NANO LETTERS

2007
Vol. 7, No. 8
2452−2458

Templating Water Stains for Nanolithography

Wei-Ssu Liao, Xin Chen, Jixin Chen, and Paul S. Cremer*

Department of Chemistry, Texas A&M University, College Station, Texas 77843

Received May 21, 2007; Revised Manuscript Received June 18, 2007

ABSTRACT

Herein, a nanoscale patterning technique is demonstrated for creating twin features in polymers and metals. The process works by combining evaporative staining with a templating process. Well-ordered hexagonally arrayed double rings were fabricated using hydrophobic spherical templates. The diameter of the rings, the width of individual rings, and the spacing between concentric and adjacent rings could be tuned by varying the solution conditions. Arrays could be made without the outer ring by employing hydrophilic templates.

Introduction. Well-defined nanoscale features have received substantial interests from scientists and engineers because of their potential applications in photonics,[1−2] electronics,[3] material science,[4] and biotechnology.[5−10] A variety of methods now exist to create nanoscale structures.[11−18] For example, photolithography provides a top-down method for creating large areas of well-defined features.[11] The capabilities of conventional photolithography are, however, typically restricted to the diffraction limit of light (>100 nm). On the other hand, electron-beam lithography is able to create features of nearly arbitrary two-dimensional geometry on a scale below 100 nm.[12] Despite its high resolution, e-beam lithography is time-consuming when large arrays are required. Moreover, the process must take place at a dedicated facility in a vacuum environment with relatively expensive equipment. These restriction have motivated the search for alternative pathways to fabricating large areas of ordered patterns.[19−21]

Irreversible solvent evaporation has recently been employed to create patterns via the dynamic self-assembly of nonvolatile dispersed solute particles.[22−24] This technique has been used to make intricate patterns, but with random size, spacing, and periodicity. Precise control over feature morphology has been very difficult to achieve because of instabilities in the evaporation process.[25] On the other hand, concentric micrometer-size patterns can be formed through the solvent evaporation process using a sphere-on-flat geometry combined with repetitive stick-slip motion under the control of a motor.[26−28] These nonconventional patterning techniques provide an alternative route for fabricating large area features. Nevertheless, the use of the solvent evaporation process under well-controlled conditions for nanoscale patterning is still a major challenge.

Template-based techniques have provided a very easy and inexpensive way to fabricate nanoscale structures.[19,21,29−39] These techniques use nanospheres,[19,21,29−33] nanoporous anodic aluminum oxide (AAO),[34−37] nanochannels,[15,38] or nanoholes[39] as templates. They can typically be combined with chemical vapor deposition,[19,29,33] ion-beam bombardment,[31,34−35,38] edge spreading,[21] electrochemical deposition,[37,39] selective wetting,[30,32] and photoreduction[36] methods to fabricate nanoscale structures. Under precise template confinement, these techniques can easily fabricate large areas with minute features. We therefore reasoned that it might be possible to combine solvent evaporation with a templating approach to design a simple, yet powerful new nanoscale patterning technique.

Herein we demonstrate the use of water stain lithography (WSL) to create large areas of twin features. Arrays of nanoscale double rings could be produced by localized solute accumulation during the solvent evaporation process by using self-assembled polystyrene spheres as templates. The double-ring structures could be formed in about 90 min with very simple equipment. Line widths under 30 nm were achieved with this method. The specific geometry of double-ring features could be precisely controlled by varying solution conditions during fabrication (Figure 1). This included the center-to-center distance between double rings (D), the radii of the rings (r_1 and r_2), the gap size between concentric rings (d), and the width of the individual rings (w_1 and w_2). It was even possible to eliminate the presence of the outer ring.

Our procedure for making hexagonally arrayed patterns of nanoscale double-rings is outlined in Figure 2. First, a thin layer of photoresist was spin-coated on top of a supporting substrate. Next, a polystyrene sphere suspension solution was introduced in a dropwise fashion on top of the polymer. The solution was an aqueous/organic mixture, which served to soften the photoresist surface.[40] The whole

* Author to whom correspondence should be addressed. E-mail: cremer@mail.chem.tamu.edu.

10.1021/nl071195c CCC: $37.00
Published on Web 07/18/2007

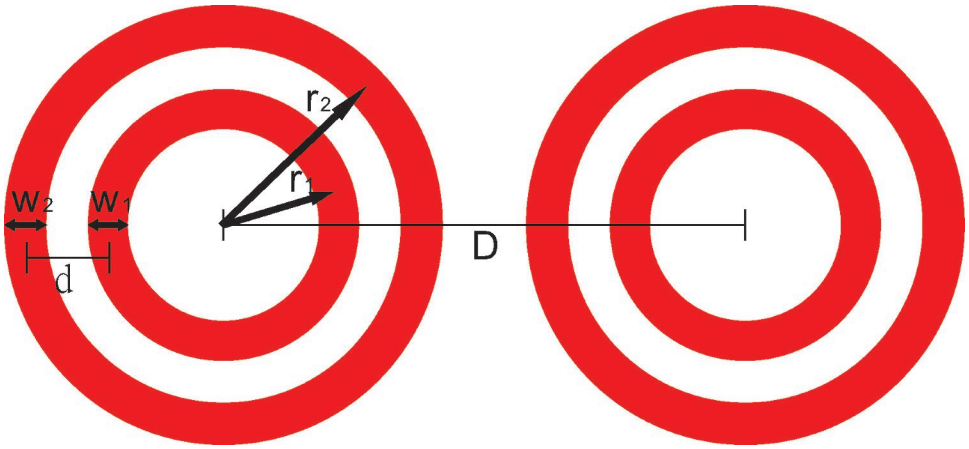

Figure 1. Parameters for double-ring features.

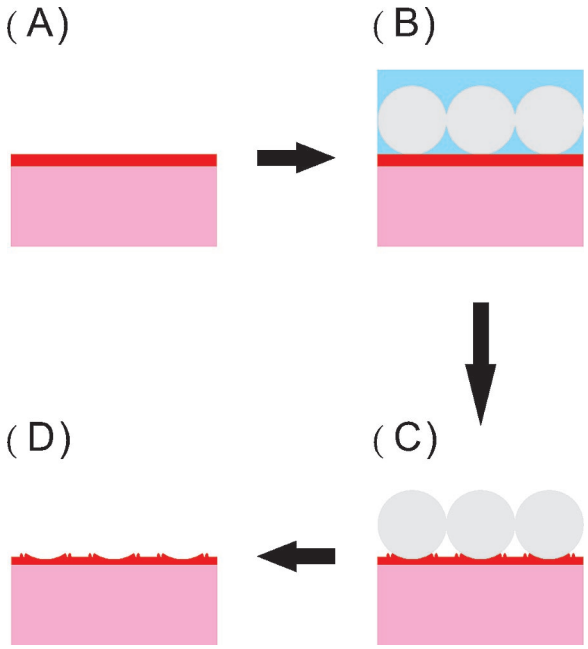

Figure 2. Schematic diagram of the process for fabricating double-ring features. (A) Spin-coating a thin layer of polymer onto a substrate. (B) Polystyrene spheres are spread on top of the chip. (C) The chip is allowed to dry under ambient conditions. (D) The spheres are removed by sonication under water.

chip was then allowed to dry under ambient conditions. After the solution evaporated from the surface, the polystyrene spheres were removed by sonication in pure water and the hexagonally arranged double-ring features remained impressed in the underlying film. The entire process could be completed within 90 min without any additional instruments.

Forming Double Rings. To perform double-ring array patterning, a stock polymer solution of Shipley 1805 (Microchem, MA) was diluted by Thinner P solution (Microchem, MA) to a 1:5 volumetric ratio in a first step. Five drops of the solution were spread on top of a 1 in. × 1 in. Au-coated glass slide and spin-coated at 2000 rpm for 2 min. Following this, the polymer coated chip was baked at 90 °C for 1 min, ramped to 120 °C for another 1 min, and then allowed to cool to ambient temperature. This created a polymer layer with a thickness of ∼100 nm on top of the substrate. The thickness was verified by measuring the depth of a scratch on the polymer surface with an atomic force microscope (AFM). After the chip cooled to room temperature, a 10.0 μL solution containing suspended monodisperse polystyrene spheres (Duke Scientific, CA) was mixed with a 10.0 μL aqueous solution containing 20% acetone by volume. This final mixture (10% acetone by volume) was introduced dropwise onto the surface. Four particle sizes were employed: 600 nm, 800 nm, 1 μm, and 2 μm.

The solvent was allowed to completely evaporate under ambient conditions over the course of 1 h. This should leave a monolayer of hexagonally close-packed polystyrene spheres behind on the surface[41−42] and such packing was confirmed by AFM. At this point, the polystyrene spheres were removed by bath sonication in deionized water for 5 min. The samples were dried and then imaged by AFM (Figure 3). As can be seen in these 5 μm × 5 μm images, well-defined double-ring features were obtained with high resolution. The features formed hexagonal arrays with a characteristic lattice spacing of (A) 2 μm, (B) 1 μm, (C) 800 nm, and (D) 600 nm, which corresponded exactly to the size of the polystyrene spheres from which they were templated. The diameters of the double ring features, however, were significantly smaller. For example, for the 800 nm lattice spacing (Figure 3C), the inner (D_{inner}) and outer (D_{outer}) ring diameters were 217 and 309 nm, respectively. The inner and outer rings, therefore, had an aspect ratio of ∼0.27 and ∼0.39 with respect to the 800 nm template sphere. The gap between the two rings was 48 nm and the thickness of each ring was 33 nm. Interestingly, the aspect ratio between the ring diameters and the template sphere diameter remained unchanged within experimental error for all sphere sizes. The average aspect ratio obtained at all sizes was of 0.28 ± 0.03 for the inner ring and 0.41 ± 0.03 for the outer ring. Therefore, the ratio of the diameters for the outer and the inner ring must also remain constant (D_{outer}/D_{inner} ∼ 1.46) and both rings should be regarded as replicas of the template spheres.

The quality of the double ring patterns remained high over macroscopic dimensions (∼1 cm^2). This lithographic technique, however, is subject to the same types of defects found in all assays, which employ monolayers of hexagonally

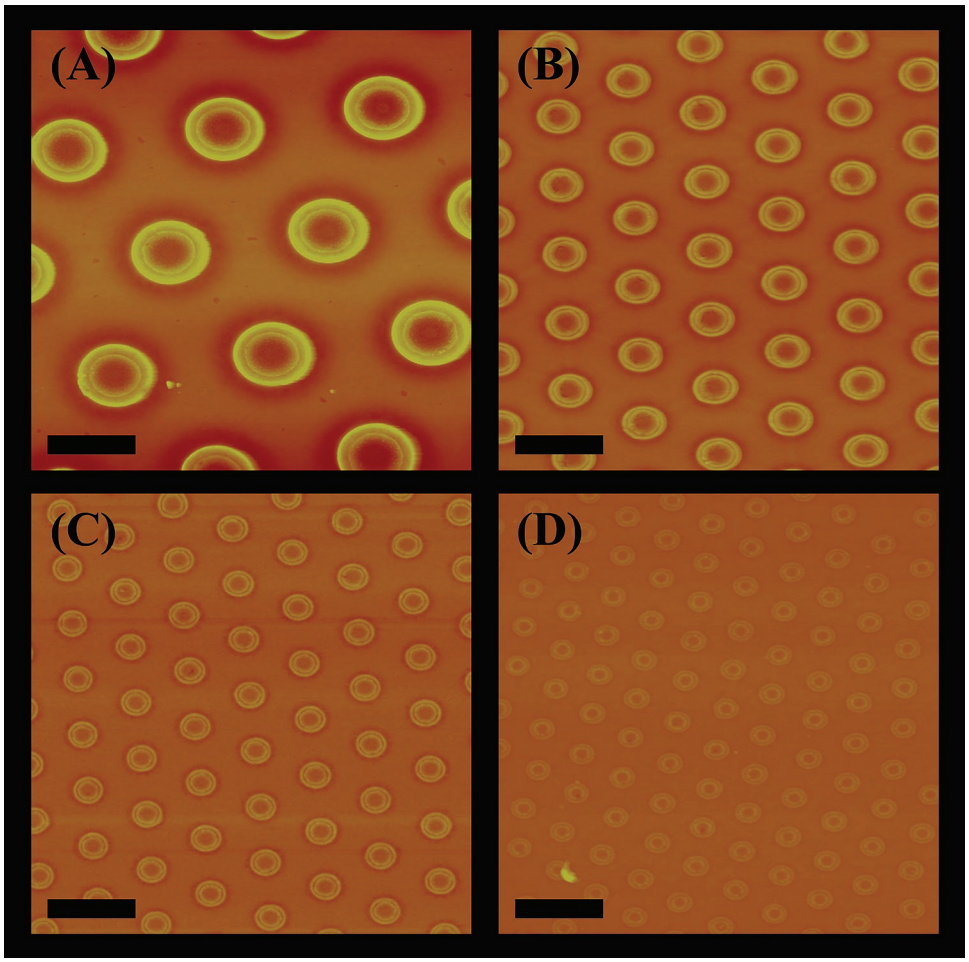

Figure 3. AFM images (5 μm $\times$ 5 μm) of double-ring features fabricated by applying polystyrene spheres of varying diameters: (A) 2 μm, (B) 1 μm, (C) 800 nm, and (D) 600 nm. Scale bars: 1 μm.

packed spherical particles. Namely, missing features are occasionally observed as well as line defects.[43] The domain size for well-ordered double ring arrays in the present experiments were approximately 25 μm $\times$ 25 μm. The details of individual double rings can still be made out in 10 μm $\times$ 10 μm images when the template sphere diameters are 1 μm or larger (Figure 4). It is, however, difficult to discern individual double-ring features from images with significantly wider fields of view because of the narrow width of individual rings as well as the small gap between them.

Controlling the Gap. The gap, *d*, between the two concentric rings could be fine-tuned by adjusting the acetone concentration in the polystyrene sphere suspension solution. Figure 5 shows a series of 2 μm $\times$ 2 μm AFM images as the concentration of acetone is increased stepwise from 0 to 30% by volume. In this case, the size of the template spheres was fixed at 800 nm. The height of the outer and inner rings increased substantially with acetone concentration. Moreover, the width of the inner ring also expanded, while the position of the outer ring showed less dramatic changes. This meant the gap between the inner and outer ring shrank with increasing acetone concentration. Without acetone, the interval between rings was 94 nm, as shown in Figure 5A. As the acetone concentration increased, this distance narrowed to 48 nm for 10% acetone and to 38 nm for 20% acetone. At 30% acetone, the inner and outer rings essentially merged together, which left a single ring with a thicker width as shown in Figure 5D. The hexagonal geometry of the double rings, however, remained unaffected. This was expected because the array spacing was inherited from the hexagonal packing of the template spheres, which was unaffected by acetone concentration.

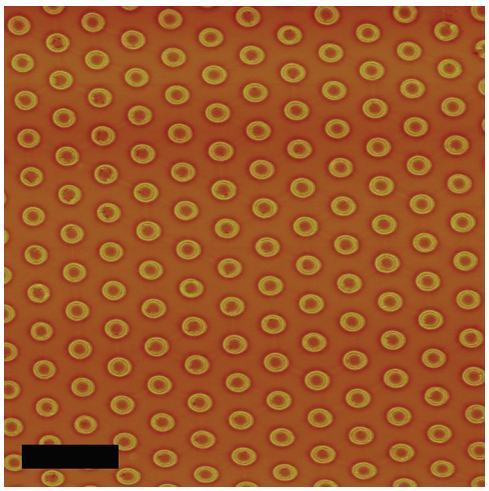

Figure 4. AFM image (10 μm $\times$ 10 μm) of double-ring features fabricated by applying 1 μm polystyrene spheres. Scale bar: 2 μm.

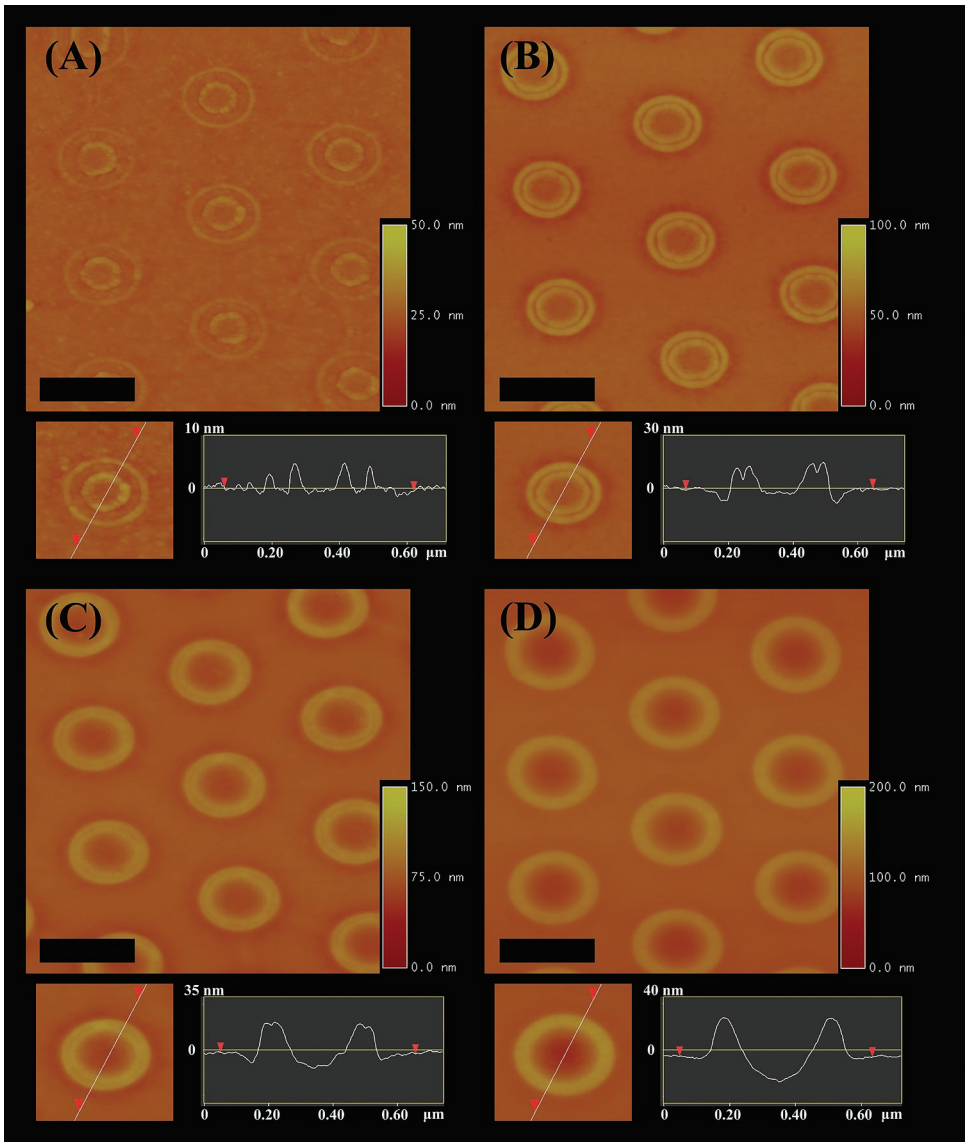

Figure 5. Series of 2 μm × 2 μm AFM images showing the effect of acetone concentration on double rings formed from 800 nm polystyrene spheres with (A) 0%, (B) 10%, (C) 20%, and (D) 30% acetone by volume. Scale bars: 500 nm.

Forming Single-Ring Features. A critical aspect of forming double-ring features involves the use of hydrophobic template spheres. If hydrophilic silica spheres were used instead, then only single rings were formed. Figure 6 shows a side-by-side comparison of results for 1 μm spherical templates of polystyrene and silica. Both samples were made from solutions containing 10% acetone by volume. A double-ring array was formed from the polystyrene spheres, but silica spheres yielded single-ring features. Significantly, the diameters of the single rings matched those of the inner ring from polystyrene. It should be noted that we also tried different substrate materials such as SU-8 and polyethylmethacrylate instead of Shipley 1805. In each case, double-ring features were obtained when using polystyrene spheres, but single rings were formed when silica spheres were employed.

Mechanism for Double Ring Formation. The data in Figures 3−6 suggest that the inner and outer rings of individual double-rings were produced by two different mechanisms. A schematic representation of our proposed ring formation mechanism with polystyrene spheres is shown in Figure 7A. In this model, the use of a dilute acetone solution leads at first to a slight amount of material being dissolved from the spin-coated Shipley 1805 layer. As the solvent evaporates, the acetone/water solution becomes saturated with polymer. The last stage of evaporation leads to polymer precipitation back onto the substrate. The precipitation is localized to the region around the base of the polystyrene spheres because this is the last location from which solvent evaporates. Such a process should form the outer ring in a manner analogous to the phenomenon by which coffee becomes enriched at the outer edge of a coffee stain.[22−24]

By contrast, the inner ring is most likely the result of a surface tension effect. This idea is consistent with the observation that the inner edge of the inner ring outlines a segment of a circle that has a diameter that corresponds quite well to that of the template spheres (Figure 7B). Therefore, the inner ring appears to be formed when acetone softens

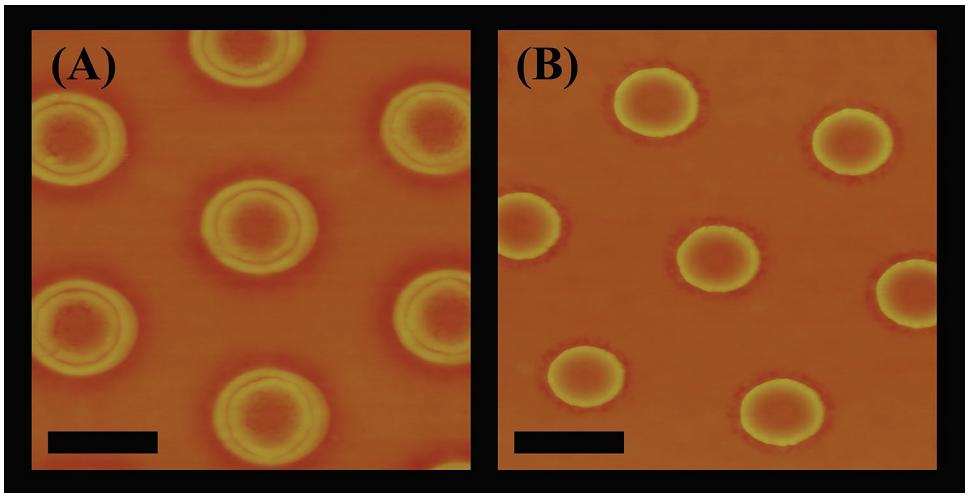

Figure 6. AFM images (2 μm $\times$ 2 μm) of polymer features fabricated by (A) 1 μm polystyrene and (B) 1 μm silica spheres. Scale bar: 500 nm.

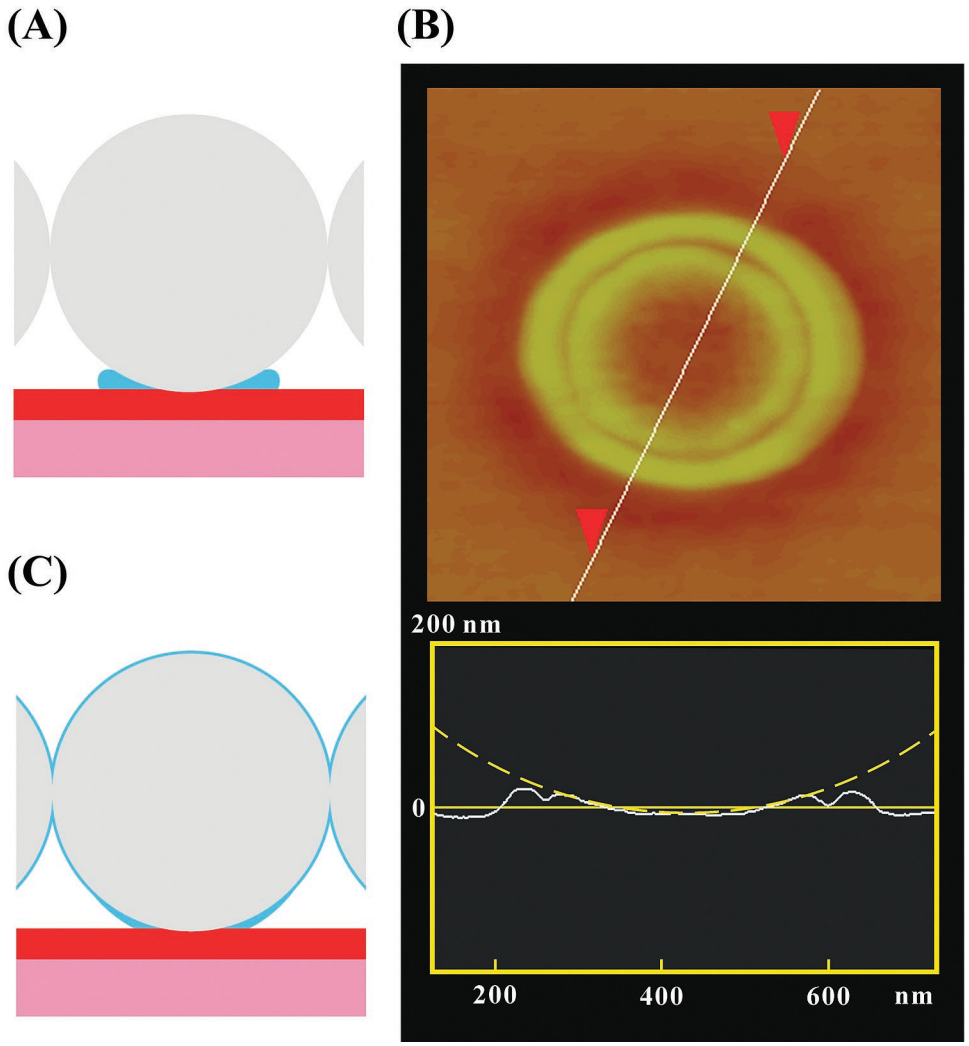

Figure 7. (A) Schematic diagram of the putative final step of the templated evaporation process with polystyrene spheres. (B) AFM image and line profile of one double-ring feature fabricated by a 1 μm polystyrene sphere. The dashed yellow line is an overlay of the outline of a 1 μm sphere on the line profile. (C) The putative final step of the templated evaporation process with silica spheres.

the photoresist layer and allows the polymer sphere to partially mold around it. This presumably occurs because it lowers the surface energy at the solvent/substrate interface.

The effect of acetone concentration provides corroborating evidence for the proposed double-ring formation mechanism. Acetone is a better solvent for Shipley 1805 than water.

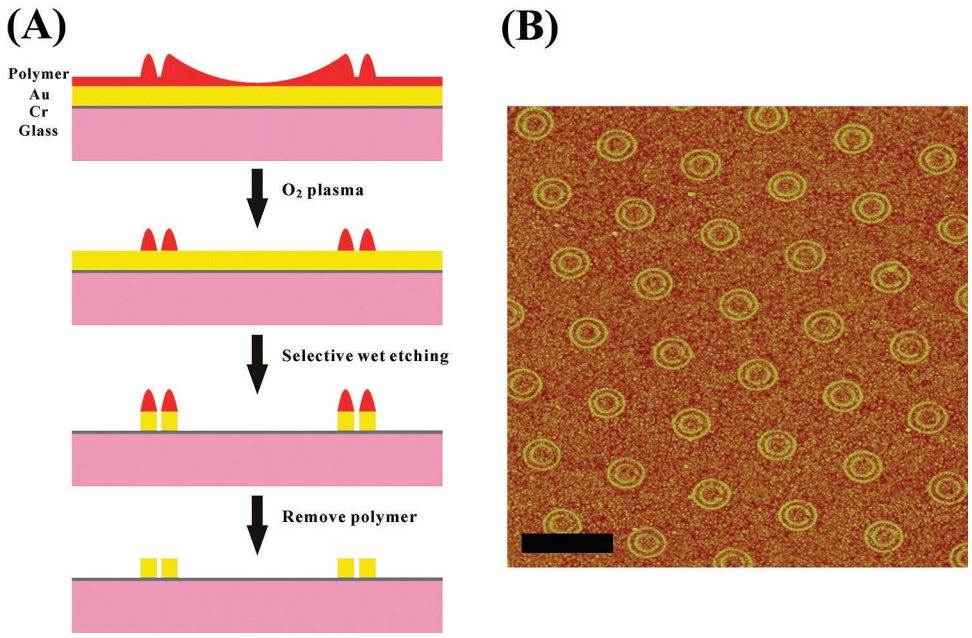

Figure 8. (A) Schematic diagram of Au double-ring formation. (B) AFM image (5 μm × 5 μm) of hexagonally arrayed Au double rings fabricated from 1 μm polystyrene spheres. Scale bar: 1 μm.

Therefore, more material should dissolve into solution as the acetone concentration is increased. Consequently, more material precipitates from solution upon solvent evaporation. This causes an increase in mass to be found at the outer ring. The higher acetone concentration also leads to a greater softening of the photoresist layer. This in turn causes the polystyrene spheres to mold more deeply into the spin-coated film. Both of these effects cause increases in feature height, and the deeper embedding of the spheres leads to a shrinking of the gap between the rings, as can be seen from the line profiles in Figure 5.

Both the polystyrene spheres and the underlying photoresist substrate were hydrophobic. This should cause a liquid toroid to form uniformly around the base of the sphere during the last step of solvent evaporation (Figure 7A). However, when silica was employed instead, the final stage of the drying process should be markedly different. In this case, the remaining liquid should preferentially coat the silica spheres and avoid the hydrophobic substrate (Figure 7C). Under these circumstances, the photoresist precipitated out onto the spheres. Once the spheres were sonicated away, the material left on the surface would be expected to shadow its original dimensions.

Forming Gold Double Rings. Polymeric double-ring arrays could be employed as templates to create corresponding features in an underlying metal film. As a demonstration, we transferred double-ring features to a gold layer. The idea is shown schematically in Figure 8A. First, double-ring features were fabricated in photoresist on top of a Au film. For this purpose, a 20 nm Au layer was evaporated onto a 3 nm thick Cr layer coated onto a glass substrate (BOC Edwards Auto 306 metal evaporation chamber). A 1:20 dilution of Shipley 1805 photoresist was coated onto the surface to a thickness of 20 nm and 1 μm polystyrene spheres were used as the evaporation templates. The solvent was pure water.

After the formation of the polymeric features, the chip was dried and placed into a 25 W oxygen plasma for 32 s with 0.2 Torr O_2. This should uniformly remove the outer most layers of photoresist. In fact, photoresist should only remain in raised locations where templating had taken place. At this point, the chip was immersed into a 1:200 (volumetric) diluted aqueous Au etching solution (NaI/I_2) for 40 s to conduct a wet chemical etch. Finally, the chip was washed with copious amounts of deionized water and acetone to remove the photoresist. This procedure should leave only gold rings on the surface. In fact, AFM imaging revealed a hexagonal array of double rings on the surface (Figure 8B). The width of each ring was 29 nm. The outer ring had a diameter of 384 nm, while the inner ring diameter was 238 nm. The spacing between concentric rings was 73 nm, and the adjacent ring distance was 1 μm.

Conclusions. We have demonstrated a simple patterning technique, water stain lithography, to fabricate well-ordered nanoscale single- and double-ring features in photoresist and Au. The ring size and spacing could be controlled by tuning the size of the template spheres and adjusting the acetone concentration in solution. This technique provides the possibility to fabricate large arrays of patterned features in a highly reproducible fashion with line widths well below 100 nm. Although spherical templates were used in these experiments, other shapes such as elongated nanorods should also be possible. We are currently studying the plasmonic, magnetic, and biosensing properties of twin features.

Acknowledgment. We thank the Robert A. Welch Foundation (grant A-1421), the Army Research Office (W911NF-05-1-0494), DARPA (FA9550-06-C-0006), and the NIH (R01 GM070622) for support.

References

(1) Joannopoulos, J. D.; Villeneuve, P. R.; Fan, S. H. *Nature* **1997**, *386*, 143.

(2) Joannopoulos, J. D.; Meade, R. D.; Winn, J. N. *Photonic Crystals: Modeling the Flow of Light*; Princeton University Press: Princeton, NJ, 1995.
(3) Jacobs, H. O.; Whitesides, G. M. *Science* **2001**, *291*, 1763.
(4) Thurn-Albrecht, T.; Schotter, J.; Kastle, C. A.; Emley, N.; Shibauchi, T.; Krusin-Elbaum, L.; Guarini, K.; Black, C. T.; Tuominen, M. T.; Russell, T. P. *Science* **2000**, *290*, 2126.
(5) Haes, A. J.; Van Duyne, R. P. *J. Am. Chem. Soc.* **2002**, *124*, 10596.
(6) Ostuni, E.; Chen, C. S.; Ingber, D.; Whitesides, G. M. *Langmuir* **2001**, *17*, 2828.
(7) Lee, K.-B.; Park, S.-J.; Mirkin, C. A.; Smith, J. C.; Mrksich, M. *Science* **2002**, *295*, 1702.
(8) Kohli, P.; Harrell, C. C.; Cao, Z.; Gasparac, R.; Tan, W.; Martin, C. R. *Science* **2004**, *305*, 984.
(9) Chan, W. C. W.; Nie, S. *Science* **1998**, *281*, 2016.
(10) Han, M.; Gao, X.; Su, J. Z.; Nie, S. *Nat. Biotechnol.* **2001**, *19*, 631.
(11) Moreau, W. M. *Semiconductor Lithography*; Plenum: New York, 1989, Chapter 8.
(12) Sze, S. M. *VLSI Technology*; McGraw-Hill: Singapore, 1988; Chapter 4.3.
(13) Dändliker, R.; Gray, S.; Clube, F.; Herzig, H. P.; Vökel, R. *Microelectron. Eng.* **1995**, *27*, 205.
(14) Gale, M. T.; Rossi, M.; Pedersen, J.; Schutz, H. *Opt. Eng.* **1994**, *33*, 3556.
(15) Martin, C. R. *Science* **1994**, *266*, 1961.
(16) Piner, R. D.; Zhu, J.; Xu, F.; Hong, S.; Mirkin, C. A. *Science* **1999**, *283*, 661.
(17) Wu, M.-H.; Whitesides, G. M. *Appl. Phys. Lett.* **2001**, *78*, 2273.
(18) Wu, M.-H.; Paul, K. E.; Whitesides, G. M. *Appl. Opt.* **2002**, *41*, 2575.
(19) Hulteen, J. C.; Van Duyne, R. P. *J. Vac. Sci. Technol., A* **1995**, *13*, 1553.
(20) Guo, Q.; Teng, X.; Yang, H. *Nano Lett.* **2004**, *4*, 1657.
(21) McLellan, J. M.; Geissler, M.; Xia, Y. *J. Am. Chem. Soc.* **2004**, *126*, 10830.
(22) Deegan, R. D.; Bakajin, O.; Dupont, T. F.; Huber, G.; Nagel, S. R.; Witten, T. A. *Nature* **1997**, *389*, 827.
(23) Deegan, R. D. *Phys. Rev. E* **2000**, *61*, 475.
(24) Deegan, R. D.; Bakajin, O.; Dupont, T. F.; Huber, G.; Nagel, S. R.; Witten, T. A. *Phys. Rev. E* **2000**, *62*, 756.
(25) Rabani, E.; Reichman, D. R.; Geissler, P. L.; Brus, L. E. *Nature* **2003**, *426*, 271.
(26) Hong, S. W.; Xu, J.; Xia, J.; Lin, Z. Q.; Qiu, F.; Yang, Y. L. *Chem. Mater.* **2005**, *17*, 6223.
(27) Xu, J.; Xia, J.; Hong, S. W.; Lin, Z. Q.; Qiu, F.; Yang, Y. L. *Phys. Rev. Lett.* **2006**, *96*, 066104.
(28) Hong, S. W.; Xu, J.; Lin, Z. Q. *Nano Lett.* **2006**, *6*, 2949.
(29) Hulteen, J. C.; Treichel, D. A.; Smith, M. T.; Duval, M. L.; Jensen, T. R.; Van, Duyne, R. P. *J. Phys. Chem. B* **1999**, *103*, 3854.
(30) Xu, H.; Goedel, W. A. *Angew. Chem., Int. Ed.* **2003**, *42*, 4696.
(31) Zhu, F. Q.; Fan, D.; Zhu, X.; Zhu, J. G.; Cammarata, R. C.; Chien, C. L. *Adv. Mater.* **2004**, *16*, 2155.
(32) Yan, F.; Goedel, W. A. *Nano Lett.* **2004**, *4*, 1193.
(33) Kosiorek, A.; Kandulski, W.; Glaczynska, H.; Giersig, M. *Small* **2005**, *1*, 439.
(34) Hobbs, K. L.; Larson, P. R.; Lian, G. D.; Keay, J. C.; Johnson, M. B. *Nano Lett.* **2004**, *4*, 167.
(35) Wang, Z. K.; Lim, H. S.; Liu, H. Y.; Ng, S. C.; Kuok, M. H.; Tay, L. L.; Lockwood, D. J.; Cottam, M. G.; Hobbs, K. L.; Larson, P. R.; Keay, J. C.; Lian, G. D.; Johnson, M. B. *Phys. Rev. Lett.* **2005**, *94*, 137208.
(36) Liao, W.-S.; Yang, T.; Castellana, E. T.; Kataoka, S.; Cremer, P. S. *Adv. Mater.* **2006**, *18*, 2240.
(37) Nicewarner-Peña, S. R.; Freeman, G. R.; Reiss, B. D.; He, L.; Peña, D. J.; Walton, I. D.; Cromer, R.; Keating, C. D.; Natan, M. J. *Science* **2001**, *294*, 137.
(38) Pearson, D. H.; Tonucci, R. J.; Bussmann, K. M.; Bolden, E. A. *Adv. Mater.* **1999**, *11*, 769.
(39) Ji, R.; Lee, W.; Scholz, R.; Gösele, U.; Nielsch, K. *Adv. Mater.* **2006**, *18*, 2593.
(40) Kim, E.; Xia, Y.; Zhao, X. M.; Whitesides, G. M. *Adv. Mater.* **1997**, *9*, 651.
(41) Deckman, H. W.; Dunsmuir, J. H. *Appl. Phys. Lett.* **1982**, *41*, 377.
(42) Deckman, H. W.; Dunsmuir, J. H. *J. Vac. Sci. Technol., B* **1983**, *1*, 1109.
(43) Haes, A. J.; Haynes, C. L.; McFarland, A. D.; Schatz, G. C.; Van Duyne, R. P.; Zou, S. *MRS Bull.* **2005**, *30*, 368.

NL071195C